Structural Engineering and Mechanics, *Vol. 72, No. 2 (2019) 191-201*
DOI: https://doi.org/10.12989/sem.2019.72.2.191

Femoral Fracture load and damage localization pattern prediction based on a quasi-brittle law

Zahira Nakhli[1a], Fafa Ben Hatira[*1] and Martine Pithioux[2,3], Patrick Chabrand[2,3] and Khemais Saanouni[4]

[1]Laboratoire de Recherche Matériaux Mesures et Application (MMA), LR11ES25, National Institute of Sciences and Technology (INSAT), 676 INSAT Centre Urbain Nord, Tunis Cedex 1080, Tunisia
[2]Aix Marseille University, UMR CNRS 7287, (ISM) Institute of Movement Sciences, Jardin du Pharo, 58 Boulevard Charles Livon, 13007 Marseille, France
[3]APHM, Sainte-Marguerite Hospital, Institute for Locomotion, Department of orthopaedics and Traumatology, 20 Avenue Viton, 13009 Marseille, France
[4]Laboratoire des Systèmes Mécaniques et d'Ingénierie Simultanée Institut Charles Delaunay, UMR CNRS 6281, UTT, TROYES, France

(Received July 24, 2018, Revised April 3, 2019, Accepted May 29, 2019)

Abstract. Finite element analysis is one of the most used tools for studying femoral neck fracture. Nerveless, consensus concerning either the choice of material characteristics, damage law and /or geometric models (linear on nonlinear) remains unreached. In this work, we propose a numerical quasi-brittle damage model to describe the behavior of the proximal femur associated with two methods to evaluate the Young modulus. Eight proximal femur finite elements models were constructed from CT scan data (4 donors: 3 women; 1 man). The numerical computations showed a good agreement between the numerical curves (load – displacement) and the experimental ones. A very encouraging result is obtained when a comparison is made between the computed fracture loads and the experimental ones (R2=0.825, Relative error =6.49%). All specific numerical computation provided very fair qualitative matches with the fracture patterns for the sideway fall simulation. Finally, the comparative study based on 32 simulations adopting linear and nonlinear meshing led to the conclusion that the quantitatively results are improved when a nonlinear mesh is used.

Keywords: Sideway fall, proximal femur fracture, quasi-brittle damage, finite element analysis, fracture pattern, non-linear meshing

1. Introduction

Precast The osteoporosis disease, which is defined as a decrease in bone strength, can be estimated by bone mineral density (BMD) measuring (Briot *et al*. 2012). This pathology causes fractures in different bone structure and is classified as the most important ones affecting the femoral neck (Tellache *et al*. 2009, Curtis *et al*. 2017). It usually occurs without apparent symptoms until the provocation of the fracture. Fracture prevention of this pathology based on diagnosis can delay surgical procedures. Finite element (FE) modeling can be a reliable tool to better screen up the different factors related to bone fractures and give surgeons more reliable criteria on fracture risk factor. Some specific models were developed in mechanical to predict human proximal femur fracture and to assess the pressure distribution under physiologic loading in bone structures. Most of these models adopted Continuum damage mechanics (CDM) as a framework. These modeling often conjugate variables of different natures (scalar or tensor) to describe the damage state of material. The particular choice of damage variable influences heavily the damage model. In all the proposed formulations, damage leads to the reduction of stiffness components, not matter if the medium is initially isotropic or anisotropic. In particular in (Maire and Chaboche 1997) authors proposed to model the damaged elastic properties of composite by combining different types of variables in the framework of CDM. In addition, Ju (1990) presented a deep analyze of the isotropic and anisotropic damage variables notions in CDM. One of the conclusion stated in this work, is that isotropic fourth-order damage tensor (not a scalar damage variable) should be used to characterize the state of damage in materials even for the isotropic damage. More recently, Pituba and Lacerda (2012) presented a comparison of simplified one and two-dimensional numerical analyses using isotropic and anisotropic damage models for the concrete. Based on this study, the authors concluded that the employment of anisotropic models has some advantages in 2D analysis when compared to the isotropic leading to a more realistic numerical response.

Concerning the prediction of bone structures damage, most of proposed models fund in the literature have tried to give an answer to the solution of fracture ultimate force as well as the fracture pattern prediction with different mechanical approaches. These studies were based on linear

*Corresponding author, Ph.D.
E-mail: zeimomo@yahoo.fr
[a] Ph.D. Student,
E-mail: zahira_nakhli@yahoo.fr

http://www.techno-press.com/journals/sem&subpage=7
ISSN: 1225-4568 (Print), 1598-6217 (Online)

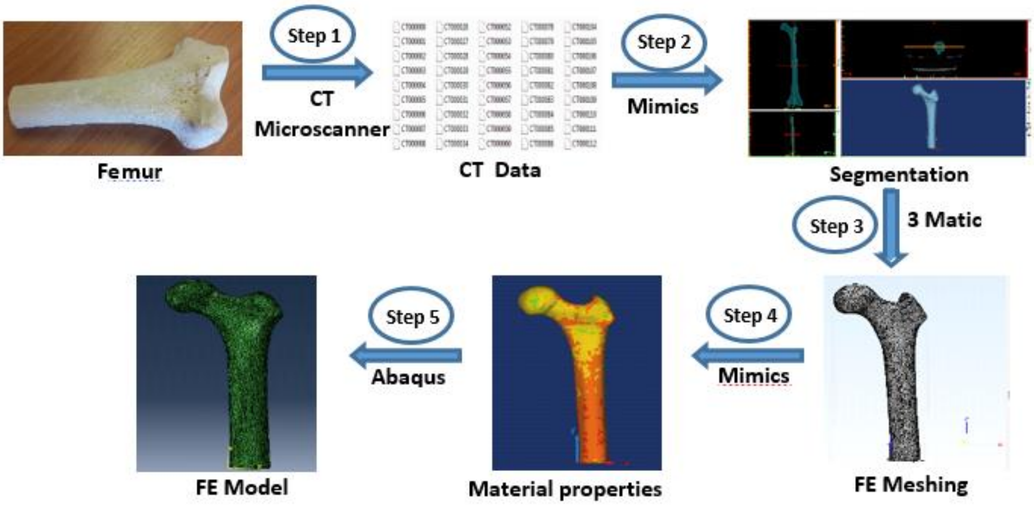

Fig. 1 The protocol established to create 3D FE Model from computed tomography data using the Hounsfield unit of CT data

and non-linear isotropic and /or anisotropic FE models (Bettamer *et al*. 2015, Viceconti *et al*. 2012, Haider *et al*. 2018, Marco *et al*. 2017, Enns-Bray *et al*. 2014, Lekadir *et al*. 2015, Zagane *et al*. 2016, Varga *et al*. 2016, Nawathe *et al*. 2015). No consensus has yet been reached, but each scientific work carried out can help to move towards a construction of an efficient prediction.

The various works mentioned above have tried to give a unique answer to the solution of modeling the behavior of bone structures and more precisely to the problem of fracture. In order to propose a new efficient numerical tool, inexpensive (from computing side of view) and of course close to experimental, a method for estimating the proximal femur fracture based on a non linear FE model is presented in this study. The Continuum Damage Mechanics CDM framework is chosen to develop the isotropic quasi-brittle fracture law with two elasticity properties (an elastic modulus proportional to the bone density ($E_{(\rho)}$) and an elastic modulus proportional to the bone volume fraction $E_{(BV/TV)}$). The model is implemented into a user routine VUMAT in the finite element software (Abaqus). The Finite element simulations were carried out using the explicit dynamic algorithm. Numerical computations for human femurs (right and left, height specimens) were compared with to experimental fracture data (values and curves) with linear and non-linear meshing.

2. Method

2.1 CT scan

Eight femurs (right and left) used in this study are coming from four donors (3 women, 1 man). The age of the donors ranged from 62 to 89 years, and averaged 79 years. Prior to preparing the femurs for the mechanical tests, CT scans were performed (scanner model: Light speed VCT 64, GE Medical System, Milwaukee, WI), with technical parameters of 120-140kV, 250-380mA. An axial scan protocol was adopted with a slice thickness of 0.625mm. The specimens were frozen to -20°C and kept until the day before the test. During the study, a calibration test was carried out using an external phantom to detect any potential drift of the instrumentation (Le Corroller *et al*. 2012). Since we know the properties of phantoms, we can deduce the properties of each point of the bone by the grey value level.

The resolution system used provides a three-dimensional map of the bone mineral density through the studied bone structures (Enns-Bray *et al*. 2014, Schmidt *et al*. 2006, Abdulkadir 2014).

The different steps taken to apply the protocol required to create the finite element model from CT data are described in Fig. 1.

The first step was the production of DICOM images files, which are generated by the scanner and constituted by pixels with different gray intensities. The second step was the 3D geometry reconstruction of each femur from the X-ray scanner images, which are based on the voxel element generation using the research software Mimics 17.0.

Densities described by grey value level were assigned to each voxel element (Dieter and Zysset 2009).The third step was the femur volume 3D mesh generating with tetrahedral elements by the research software 3Matic 9.0.0.231. In order to assign the material parameters, the volume mesh was finally imported a second time in Mimics (step 4). Thereby, a 3D model specific to each patient respecting his anatomy and possessing material properties related to the quality of his bone was created and imported to the Abaqus/CAE software (step 5). More details of this protocol can be found in previous article (Nakhli *et al*. 2017).

2.2 Experimental mechanical compression test

A simulation of a sideways fall on the greater trochanter is reproduced through a loading to failure of each proximal femur in the INSTRON 5566 machine. Femurs were fixed

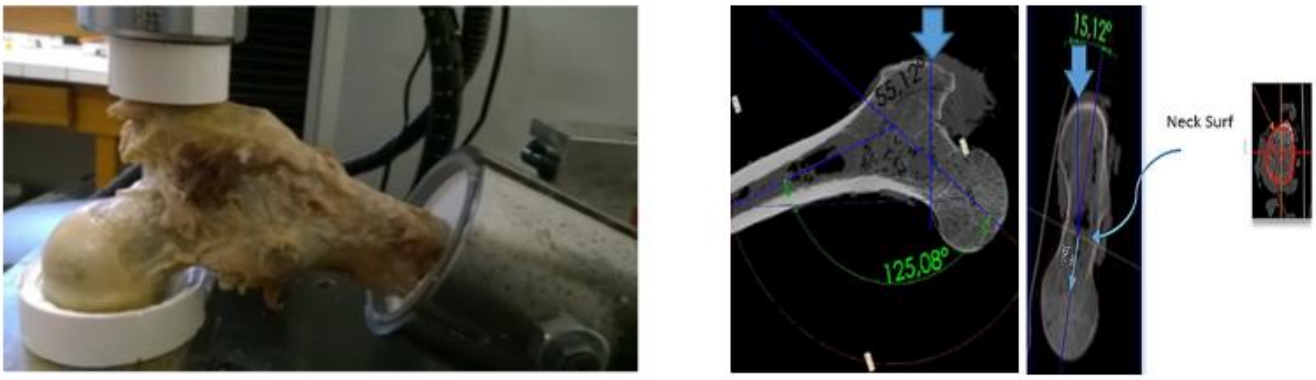

Fig. 2 The mechanical compression test conditions (left): CT scans before fracture (Right): Normal diaphysealangle125.08°, Femur was fixed in resin (Epoxy Axon F23) at 15.12° internal rotation

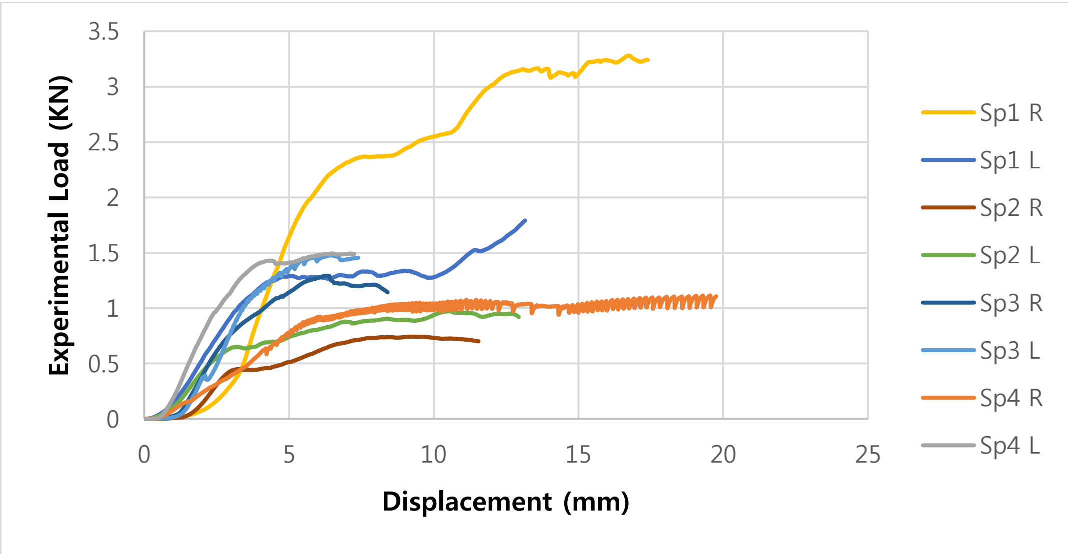

Fig. 3 Experimental load vs. displacement for the eight specimens

Table 1 Failure values for the eight proximal Femurs

Specimen	Femur	BMD (g/cm2)	Fracture Load (N)
Sp1L	Osteoporotic	0.65	1524
Sp1R	Osteoporotic	0.72	2319
Sp2L	Osteoporotic	0.62	973
Sp2R	Osteoporotic	0.51	743
Sp3 L	Osteoporotic	0.71	1477
SP3R	Osteoporotic	0.70	1293
Sp4L	healthy	0.84	1494
Sp4R	healthy	0.86	1114
Mean value		0.7	

in resin (Epoxy Axon F23) at 15.12° internal rotation. The load was applied to the greater trochanter through a pad, which simulated a soft tissue cover, and the femoral head was molded with resin to ensure force distribution over a greater surface area (Le Corroller *et al*. 2012). The Fig. 2 shows the mechanical test conditions of the sideway fall simulation. The femoral shaft was oriented at 10° adduction in the apparatus (Fig. 2 left). For this Specimen, the diaphyseal angle between the neck forms and the shaft was around 125° degrees.

The results of the different conducted experiences are reported in Table 1. It gives the details of the obtained ultimate failure load and the bone mineral density (BMD) for all femurs, (six right and left osteoporotic femurs and two healthy ones). The mean value of the BMD was found to be 0.7 g/cm2.

From experimental data, eight load-displacement curves are plotted in Fig. 3. The obtained curves for right and left femurs taken from the same donor showed different tendency with different fracture load magnitude. Exception is however reported for the curves of Specimen 2 where similarity is noticed for the left and the right femurs.

2.3 Young modulus estimation

In the present work and for the sake of comparison, bone was modelled with two mechanical properties (Young modulus E (MPa)) estimated through two different methods. These techniques were used in previous works. Indeed, most of these studies found in the literature, adopted an elastic modulus proportional to the bone density ($E_{(\rho)}$). As examples of these works, we can recall Morgan *et al*. E.F *et*

Table 2 Material Properties for height specimens

Femur		Density (g/cm3)	Young Modulus(Mpa) Method 1	Young Modulus(Mpa) Method 2	Poisson ratio
Sp1	L	0.28 - 2.45	121 - 14475	3777	0.3
	R	0.25 - 2.46	103 - 14552		
Sp2	L	0.47 - 2.44	384 - 14293		
	R	0.35 - 2.42	199 - 13991		
Sp3	L	0.41 - 2.41	292 - 13905		
	R	0.32 - 2.46	161 - 14469		
Sp4	L	0.34 - 2.46	185 - 14526		
	R	0.31 - 2.45	151 - 14405		

al. (2003), Keyak (2001), Ariza *et al*. (2015), Pithioux *et al*. (2011) and Haider *et al*. (2018). However, some researchers adopted a second method based on the assumption that the elastic modulus is a function of the ration of the bone volume (BV) to the total volume (TV) (Hambli R. *et al*. (2012) and Varga P. *et al*. (2016)). We will briefly recall here after these two methods.

Method 1: Young's modulus estimation based on bone density ($E_{(\rho)}$)

The first method using the following expression gives a varying Young modulus (E) related to the bone apparent density ρ (g/cm3) such as defined by Kaneko *et al*. (2004),

$$E_{(\rho)} = 2000(\rho)^{1.89} \tag{1}$$

This method is based on a phenomenological law and allows to assign to each element a distinct mechanical property using a direct correlation between apparent density and Young Modulus. In the end, a heterogeneous material distribution was obtained.

Method 2: Young's modulus estimation based on bone volume fraction *($E_{(BV/TV)}$)*

For method 2, we adopt the relationship based on the study of Hernandez *et al*. (2001). The Young's modulus is computed as following:

$$E_{(BV/TV)} = 84370\left(\frac{BV}{TV}\right)^{2.58} \tag{2}$$

BV/TV: bone volume/total volume fraction;

Thirty-two numerical computations based on eight Femurs reconstructions are validated through a comparison of the experimental crack localization and the estimated failure loads. The material properties E and ρ are summarized in Table 2. Poisson ratio is set at 0.3 based on the work of (Currey 1988, Carter and Hayes 1977), and BV/TV is assumed to be equal to 30% (Hambli *et al*.2012).

In the next section, a CDM model coupled with the two elastic properties is presented and will be used to reproduce the experimental data (femoral fracture loads and damage localization patterns).

2.4 Constitutive framework: A quasi brittle damage model

The approach of irreversible thermodynamics with internal variables (Krajcinovic 1989, Kachanov 1986, Saanouni *et al*. 1996) is chosen to present a coupled damage elastic order to describe the progressive initiation and propagation of cracks within human proximal femur under quasi-static load. We present hereafter the model based on Marigo (1981) quasi-brittle damage law and formulated in the Continuum Damage Mechanics (CDM) framework.

In this work, the energy based model is described throughout state variables (external and internal).The state variables describing the constitutive equations are represented by the external and the observable state variables, namely the elastic strain components $\varepsilon_{ij}{}^{e}$ and the Cauchy stress σ_{ij}.

For the sake of simplicity, damage is supposed isotropic described by a couple of scalar internal variables (D, Y) where Y is the damage force associated to the damage variable D.

The state relationships defining the stress–strain relati on of elasticity based damage mechanics can be expresse d by:

$$\sigma_{ij} = (1 - D)a_{ijkl}\varepsilon_{kl}{}^{e} \tag{3}$$

where a_{ijkl} are the components of elasticity tensor.

The damage force Y is written as:

$$Y = \frac{1}{2}\varepsilon_{ij}{}^{e}a_{ijkl}\varepsilon_{kl}{}^{e} \tag{4}$$

The damage criterion (or damage yield function) is described by:

$$f(Y, D) = Y - \frac{1}{2}Y_0 - mD^{\frac{1}{s}} = 0 \tag{5}$$

where Y_0,s and m are three parameters characterizing the damage evolution. It is here assumed that the damage yield function Eq.(5) can describe the initiation of micro-cracks starting from undamaged state (D=0).

The damage evolution equation is derived to get:

$$\dot{D} = \frac{s}{m}\left(\frac{\dot{Y}}{D^{\left(\frac{1-s}{s}\right)}}\right) \tag{6}$$

In which the time derivative of the force Y is given by:

$$\dot{Y} = \varepsilon_{ij}{}^{e}a_{ijkl}\dot{\varepsilon}_{kl}{}^{e} \tag{7}$$

According to Eq. (3), when damage increases by Eq. (6), then the stress tensor decreases due to the decrease of the elastic modulus, i.e if the critical value of damage (D=1.0) is reached, the material point is declared as fully damaged and the value of D is assumed to be 0.999 to avoid the numerical instabilities.

In the next section the details of the implementation of the model in the Abaqus/Standard software are given.

2.5 The proposed Algorithm

The proposed algorithm followed to implement the model is summarized in Fig. 4. The first step consists of the global model definition: geometry, load conditions and initial bone density distribution. The Second Step is concerned with the

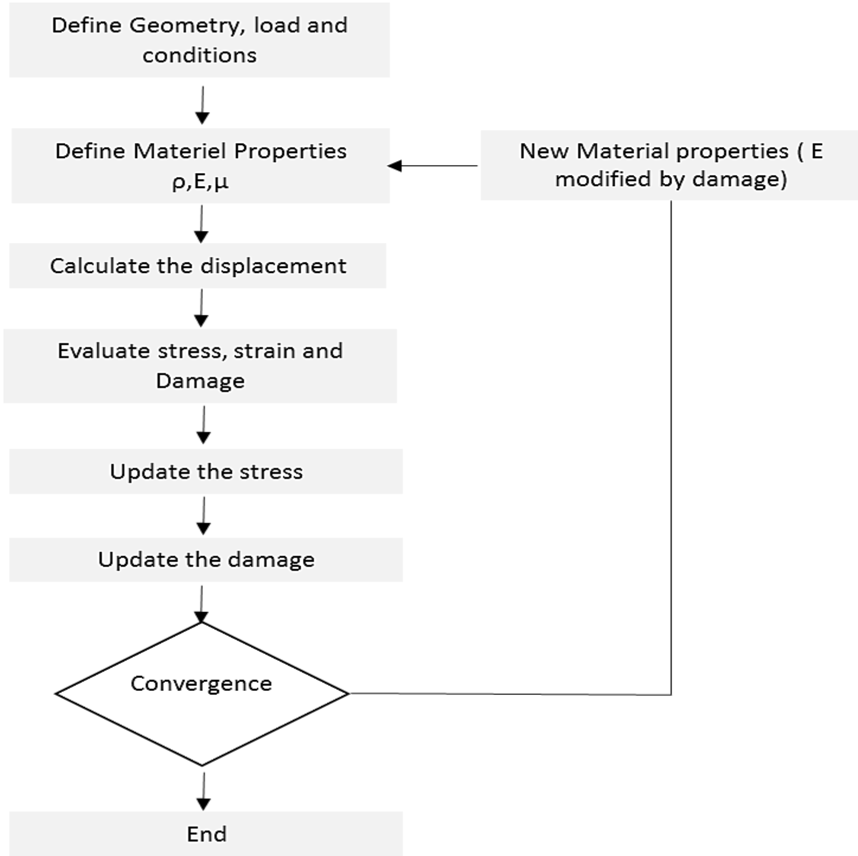

Fig. 4 Algorithm for damage modelling

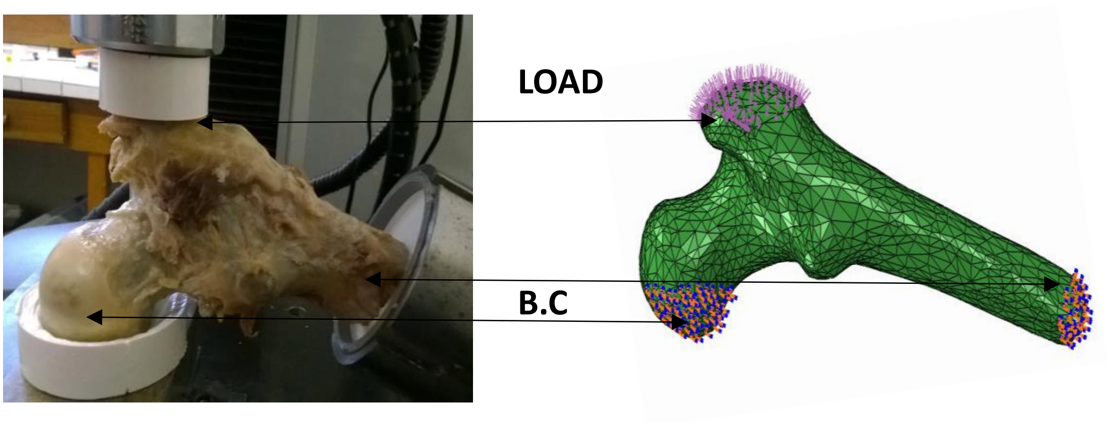

Fig. 5 The mechanical compression test conditions (Left) and BCs applied to the FE model (Right)

determination of Young's modulus, Poisson's ratio and the density. These material properties are obtained by two methods as explained in section 2.3. The third step is related to the calculation of the displacement, by solving the variational equation of the displacement field. Based on the FE method, strain, the stress and the damage are computed at each discrete location (step 4). Thereafter, an update of the stress (step 5) and damage (step 6) values are applied. The model being implemented into the subroutine VUMAT, a check for convergence is executed. The final result is obtained when the convergence criterion is satisfied; otherwise, the iterative process continues from Step 2.An illustration of the algorithm used is described in Fig. 4.

3. Simulation

Boundary and Loading conditions

The numerical validations are conducted with the boundary condition and load case matching the experimental conditions (Fig. 5). The load was applied on femoral Greater trochanter reproducing the sideway fall case, whereas the femoral head and the lower surface were constrained.

Two Types of meshes were applied for each Femur, linear tetrahedral elements (C3D4), and nonlinear quadratic tetrahedral elements (C3D10) (six degrees of freedom per node, which are the three displacements and the three rotations for both elements).

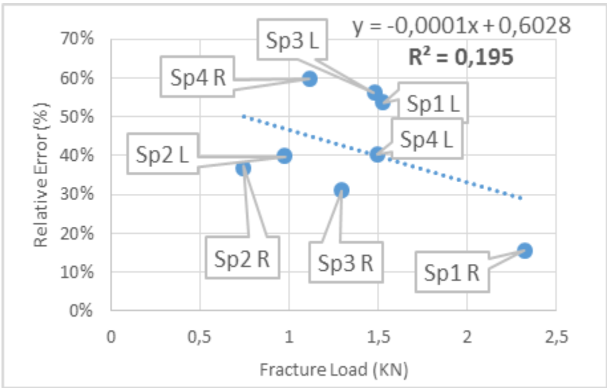

(a) Case A: Method1-Linear Mesh

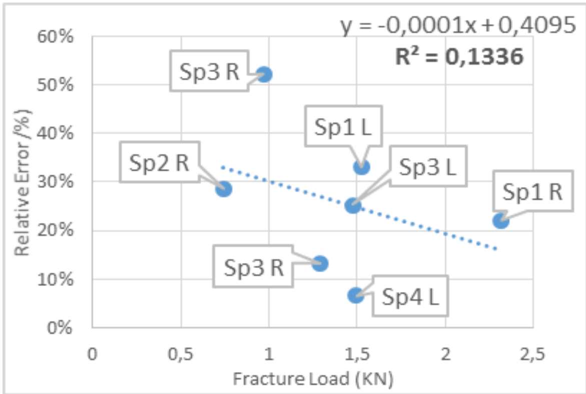

(b) Case B: Method1-NonLinear Mesh

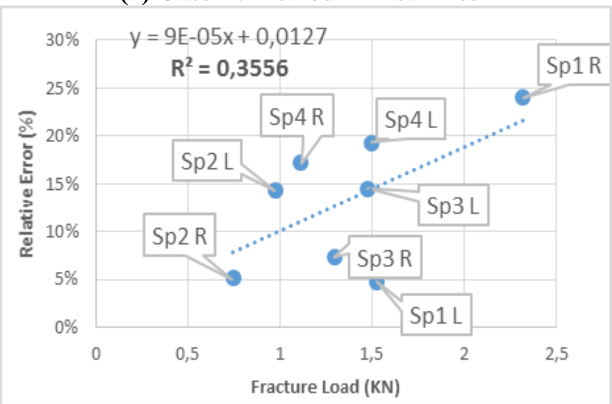

(c) Case C : Method2-Linear Mesh

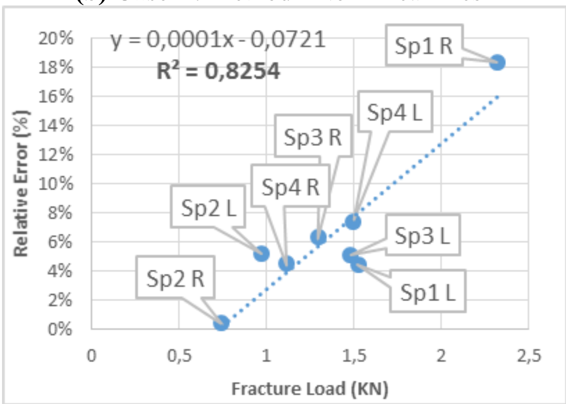

(d)Case D : Method2-NonLinear Mesh

Fig. 6 Thirty two numerical fracture loads (KN) and the relative error based on a comparison with the experimental data for the eight specimens (right and left femurs) computed with E_1 and E_2

From the numerical point of view, the crack was modelled as the region of elements where a damage growth initiates a decrease in the stress like variable (σ Cauchy stress) induced by a decrease in the material elastic properties. When element is fully damaged (D=1), the corresponding stiffness matrix is zero. Consequently, this element has no more contribution to the global stiffness.

matrix (in the case of isotropic damage (Milne 2003). This choice is necessary to ovoid divergence of the overall resolution scheme (Mariage 2004). The corresponding totally damaged elements are then "killed" from the structure, which contribute to save CPU time.

Concerning the contact problem that may occur during this numerical process, Abaqus/CAE software automatically uses a general contact algorithm to avoid intersection of the damage elements.

4. Results

The general purpose of this work is to compare the prediction of the damage localization as well as of the ultimate fracture load for different specimens tested experimentally. The analysis details the fracture load and the localized damaged zones dependency on the young modulus estimation (method 1 and method 2) as well as the linearity or not of the meshing.

The correlations between the experimental and FE computed fracture loads for the four studied cases are exposed in Fig. 6 (Case A: Method1-Linear Mesh, Case B: Method1-NonLinear Mesh, Case C: Method2-Linear Mesh, Case D: Method2-NonLinear Mesh). The relative errors between the experimental and the computed fracture loads are reported in Table 3. For each case, the relative errors are calculated for the eight femurs. In the second column of the Table 3, the minimum and maximum are noted, while in the third column the average of the relative errors for the eight femurs in the corresponding case are reported. In summary, the numerical computations based on the combination of $E_{(BV/TV)}$ and a nonlinear mesh (Case D), present the best agreement with the experimental data (fracture load magnitude) with the best correlation (R^2 = 0.825). For the other cases, correlations R^2 were found to be weak and lower than 0.356 (Fig.6). Also, an acceptable average of fracture load error was found to be 6.49 % for case D whereas an average error of 41.63 was obtained for case A (Table 3).

Table 3 Relative Error's summary

	Relative Error (%)	Average (%)
Case A	[15.6 ; 59.7]	41.63
Case B	[6.5 ; 52.2]	23.95
Case C	[4.7 ; 24]	13.31
Case D	[0.4 ; 18.4]	6.49

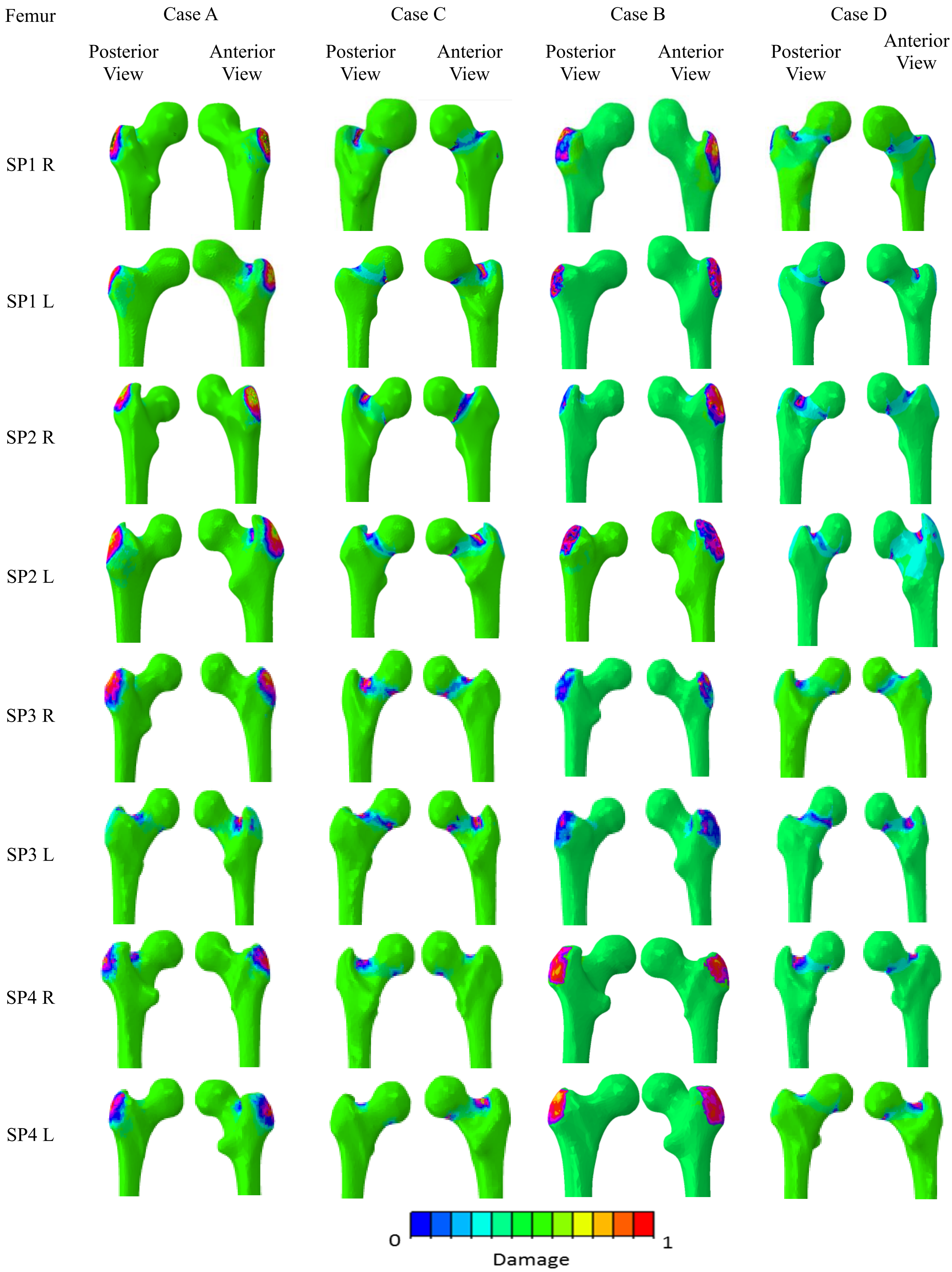

Fig 7 - Predicted fracture pattern from different view and quasi-brittle damage distribution

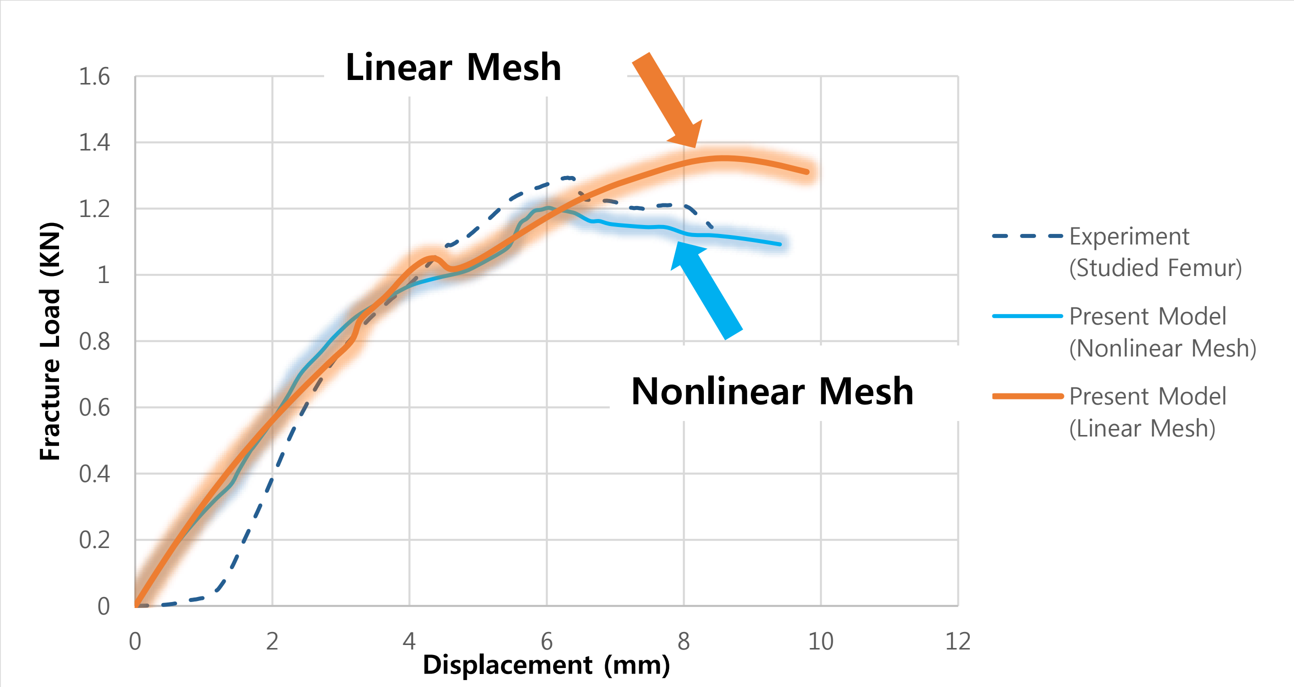

Fig. 8 Predicted and experimental force-displacement curves of the specimen (Sp3R) for the cases C and D.

These results are in agreement with previous studies such the one presented in (Sanyal 2013) where it is stated that the mechanical properties of trabecular bone depend on the material properties of bone tissue matrix, the bone volume fraction (BV/TV) and microarchitecture. It has been also shown in the same work that under uniaxial loading the variation in both compressive and shear strength was primarily attributed to the volume fraction of the trabecular bone. In this present study, the choice of an elastic modulus $E_{(BV/TV)}$ did give quite satisfactory results, evidencing the good description of femur damage fracture. They however encouraged authors to proceed with its improvement in order to include homogenization techniques proposed for complex materials as proposed in (Sanyal 2013, Pituba *et al*. 2016, Blanco *et al*. 2016, and Toro *et al*. 2016). Specifically, we can recall the study presented in (Pituba and Borges 2017) where authors proposed a computational homogenization-based approach for concrete to capture the major characteristics of the mechanical behavior of the considered quasi-brittle material. The numerical examples presented in this work showed that the proposed modelling has captured complex phenomena while adopting simple constitutive models. Finally, concerning the meshing issue, the preceding results confirm that the use of quadratic tetrahedral elements (Case D) give more accurate solution than the use of linear tetrahedral elements (Case C) as detailed in (Wang *et al*. 2004).

The propagations of the cracks and the distribution of the quasi-brittle damage of the eight femurs are plotted in Fig.7.

The results of the numerical computations gave two different crack localizations based on the choice of the elastic property. Indeed, the FE simulations performed with the method 2 showed a femoral neck (transcervical) fracture, the crack is initiated locally at the superior surface of femoral neck. In this case, the damage surface corresponded to the fracture surface observed in the experience, differently from the result obtained with method1, where fracture occurred in the Greater trochanter. The same tendency is obtained for all the studied femurs (right and the left). The crack localizations for the two models linear and nonlinear are quasi similar which demonstrate that damage pattern is not dependent on the finite element type.

Special attention will now be paid to one of the specimens presented in the previous overall results. The final goal is to better underline the quantitative and qualitative results obtained for the eight specimens. The specimen chosen is SP3R (an osteoporotic femur). It is a representative sample of all the studied specimens. A comparison between the experimental and numerical behavior curves fir the cases C and D is presented for the sideway fall numerical simulations. The results that are given in Fig. 8 show a good agreement between experimental and numerical results. The nonlinear meshing (case D) shows the best fit with experimental curve, as well as a sharp drop in force during failure.

Figs. 9(a) -(b) show that regardless of the choice of type of meshing linear (case C) or nonlinear (case D), we obtain fracture localizations similar to the ones obtained experimentally (Fig. 9(c)). The results bring the proof that the fracture line is located in the neck region. These results clearly demonstrated that the magnitude of the ultimate force is affected by the choice of the type of mesh (linear or non-linear) whereas the damage pattern does not depend on this parameter.

A shown in Fig. 10, the computations are carried out

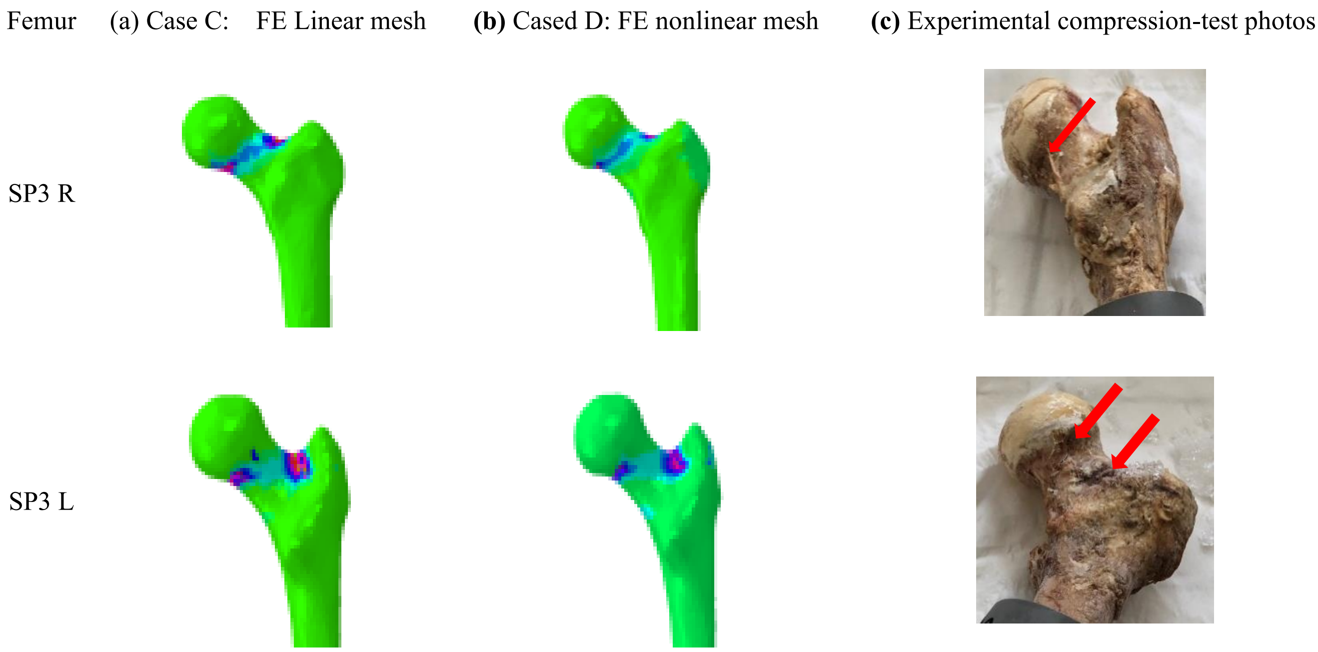

Fig. 9 Qualitative evaluation of the FE based fracture pattern prediction, showing the anterior view for specimen 3 right and left adopting method 2

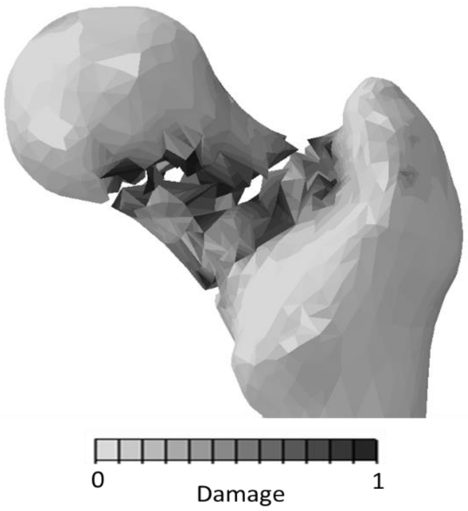

Fig.10 The complete predicted fracture pattern of the femur SP3-L (Case D) beyond the experimental ultimate load

beyond the ultimate strength, more elements are efficiently removed (killed) which demonstrate the capacity of this numerical tool to simulate a fracture process.

Further investigation have been performed to check the mesh objectivity of the computed fracture load for the studied specimen Sp3L with a choice of the Method 2. For both Cases C and D, three FEM models were built with decreasing levels of mesh refinement (Fig.11 (a)-(b)). The models will be referred to as ‘Mesh 1’, ‘Mesh 2’ and ‘Mesh 3’ throughout the text. The number of nodes and elements in each model are listed in Fig. 11(a)-(b). We can see that the distribution of the damage variable D inside the two Meshing models was the same for the three meshes but the crack width was directly correlated to the mesh size. The relative error between the experimental and numerical failure loads were fairly acceptable for the studied cases. Indeed, the relative errors δ ranges were (5,09%< δ <5,70%) and (14,50% < δ <15,24%) respectively for Nonlinear Mesh and Linear Mesh . We can conclude as far as the magnitude failure load is concerned, the element size have a weak incidence and that our numerical model can be considered as a reliable prediction tool.

5. Discussion

The aim of the present study was to conduct a comparative study based on 32 simulations. As a first remark, we can say that the predicted force-displacement curve shows the same trend as the one observed experimentally. Regarding the relative error, the average error was about 6.49% with very good fracture pattern predictions for all specimens, compared to previous works. As an example, Haider *et al*. (2018) found average percentage errors of predicted fracture load was about 9.6% and peak error of only 14%.

In general, we found statistically a good correlation between the experimentally and computationally results for the case D (R^2=0.825). However, low correlation was found between experimental and FE model for the cases A and B. Regarding the localization issue, the experimental bone failure locations were similar with the locations obtained with FE simulations for cases C and D (linear and non-linear meshing). Beside, referring to the Garden Classification (Frandsen *et al*. 1988) which is a system of categorizing intra-capsular hip fractures of the femoral neck, four different fracture types can be observed based on the bone trabeculae displacement. In this work, the fracture patterns correspond to a transervical neck fracture (type II of the Garden classification). It is characterized by a complete fracture with minimal or no displacement from anatomically normal position. To the best of the author's knowledge, this is the first time a comparison of numerical simulations with linear and nonlinear meshing were conducted to predict femoral fracture.

However, mesh sensitivity is noticed since the size of the damaged region corresponds to the size of the finite element. An efficient homogenization techniques have to be then adopted to better predict fracture load, fracture pattern, and fracture initiation. The efficiency of adaptive mesh for the crack propagation simulation proved in (Labergère *et al.* 2007) can be a starting point to treat these mesh sensitivity problems.

6. Conclusion

The purpose of this work was to develop and validate a simple FE model based on continuum damage (CDM) mechanics in order to simulate the complete force–displacement curve of femur failure. Femoral fracture load was predicted using an isotropic quasi brittle-damage FE model for thirty-two studied cases, combining two elastic modulus distribution (($E_{(\rho)}$) and ($E_{(BV/TV)}$)) with linear and nonlinear meshes. The obtained results show a strong linear relationship between FE predicted and experimentally measured fracture load (R^2= 0.825) in the case a combination of an elastic modulus related to the bone volume fraction ($E_{(BV/TV)}$) distribution with non-linear mesh is adopted. Furthermore, all eight cadaveric specimens present similar failure locations between the experimental and the FE simulation, when the method 2 is adopted.

Despite the limitations reported in the discussion, the relatively low average error in the studied cases suggests that this FE modelling may be useful in helping surgeon to choose a patient-specific treatment, and allowing them to make the right decision before the surgery by evaluating the risk factor from the fracture pattern.

Acknowledgments

The contribution of Saint Marguerite hospital radiology team specially P. Champsaur, T. Lecorroller, and D. Guenou is gratefully acknowledged.

References

Abedini, M., Khlaghi, E. A., Mehrmashhadi, J., Mussa, M. H., Ansari, M. and Momeni, T. (2017), "Evaluation of concrete structures reinforced with fiber reinforced polymers bars: A Review", *J. Asian Sci. Res.*, **7**(5), 165-175.

AbdulKadir, M.R. (2014), "Finite Element Model Construction", *Computational Biomechanics of the Hip Joint,* Springer, Berlin, Germany. 19-42.

Ariza, O., Gilchrist, S., Widmer, R.P., Guy, P., Ferguson, S.J., Cripton, P.A. and Helgason, B. (2015), "Comparison of explicit finite element and mechanical simulation of the proximal femur during dynamic drop-tower testing", *J. Biomech.,* **48**(2015), 224-232. https://doi.org/10.1016/j.jbiomech.2014.11.042.

Bettamer, A., Hambli, R., Allaoui, S. and Almhdie-Imjabber, A. (2015), "Using visual image measurements to validate a novel finite element model of crack propagation and fracture patterns of proximal femur", *Comput. Methods Biomech. Biomed. Eng: Imaging Visualization*, **5**(4), 251-262. https://doi.org/10.1080/21681163.2015.1079505.

Blanco, P.J., Sanchez, P.J., de Souza Neto. E.A. and Feijoo., R.A. (2016), "The method of multiscale virtual power for the derivation of a second order mechanical model", *Mech. Mater.*, **99**(2016), 53-67. https://doi.org/10.1016/j.mechmat.2016.05.003.

Briot, K., Cortet, B., Thomas, T., Audran, M., Blain, H., Breuil, L.C., Chapurlat, R., Fardellone, P., Feron, J.M., Gauvain, J.B., Guggenbuhl, P., Kolta, S., Lespessailles, E., Letombe, B., Marcelli, C., Orcel, P., Seret, P., Trémollière, F. and Roux, C. (2012), "Actualisation 2012 des recommandations françaises du traitement médicamenteux de l´ostéoporose post-ménopausique" , *Rev. Rhumatisme*, **79** (2012), 264-274. https://doi.org/10.1016/j.rhum.2012.02.006.

Carter, D.R., and Hayes, W.C. (1977), "The compressive behavior of bones as a two-phase porous structure", *J. Bone Joint Surg. Am.*, **59**, 954-962.

Currey, J.D., (1988), "The effect of porosity and mineral content on the Young's modulus elasticity of compact bone", *J. Biomech.*, **21**, 131-139. https://doi.org/10.1016/0021-9290(88)90006-1.

Curtis, E.M, Moon, R.J., Harvey, N.C. and Cooper, C. (2017), "The impact of fragility fracture and approaches to osteoporosis risk assessment worldwide", *Bone*, **104**, https://doi.org/10.1016/j.bone.2017.01.024.

Dannilo, C.B. and Pituba, J. (2017), "Analysis of quasi-brittle materials at mesoscopic level using homogenization model", *Adv. Concrete Construct.*, **5**(3), 221-240. https://doi.org/10.12989/acc.2017.5.3.221.

Dieter, H.P. and Zysset, P.K. (2009), "A comparison of enhanced continuum FE with micro FE models of human vertebral bodies", *J. Biomech*., **42**, 455-462. https://doi.org/10.1016/j.jbiomech.2008.11.028.

Enns-Bray, W.S., Owoc, J.S., Nishiyama, K.K. and Boyd, S.K. (2014), "Mapping anisotropy of the proximal femur for enhanced image based finite element analysis", *J. Biomech*., **47**(2014), 3272-3278. https://doi.org/10.1016/j.jbiomech.2014.08.020.

Frandsen, P.A., Andersen, E., Madsen, F. and Skjodt, T. (1988), "Garden´s Classification of femoral Neck Fractures", *J. Bone Joint Surg.*, **70B**(4), 588-590. https://doi.org/10.1302/0301-620X.70B4.3403602.

Haider, I.T., Goldak, J. and Frei, H. (2018), "Femoral fracture load and fracture pattern is accurately predicted using a gradient-enhanced quasi-brittle finite element model", *Med. Eng. Phys*, **55**, 1-8. https://doi.org/10.1016/j.medengphy.2018.02.008.

Hambli, R., Bettamer, A. and Allaoui, S. (2012), "Finite element prediction of proximal femur fracture pattern based on orthotropic behavior law coupled to quasi-brittle damage", *Med. Eng. Phys.*, **34**, 202- 210.

Hernandez, C.J., Beaupre, G.S., Keller, T.S. and Carter, D.R. (2001), "The influence of bone volume fraction and ash fraction on bone strength and modulus", *Bone*, **29**(1),74-78. https://doi.org/10.1016/S8756-3282(01)00467-7.

Ju, J.W. (1990), "Isotropic and Anisotropic damage variables in continuum damage mechanics", *J. Eng. Mech.*, **116** (12), 2764-2770. https://doi.org/10.1061/(ASCE)0733-9399(1990)116:12(2764).

Kachanov, L.M. (1986), *Introduction to Continuum Damage Mechanics*, Martinus Nijhokk Publishers, Netherlands.

Kaneko, T.S., Bell, J.S., Pejcic, M.R., Tehranzadeh, J. and Keyak, J.H. (2004), "Mechanical properties, density and quantitative CT scan data of trabecular bone with and without metastases", *J. Biomech*., **37**, 523-530. https://doi.org/10.1016/j.jbiomech.2003.08.010.

Keyak, J.H. (2001), "Improved prediction of proximal femoral fracture load using nonlinear finite element models", *Med. Eng. Phys*., **23**, 165-173. https://doi.org/10.1016/S1350-4533(01)00045-5.

Krajcinovic, D. (1989), "Damage mechanics", *Mech. Mater*., **8**, 117-197. https://doi.org/10.1016/0167-6636(89)90011-2.

Labergère, C., Rassineux, A. and Saanouni, K. (2007), "Endommagement et procédé de mise en forme. Apport du maillage adaptatif", *8e Colloque national en calcul des structures*, Giens, France, May 2007.

Le Corroller, T., Halgrin, J., Pithioux, M., Guenoun, F., Chabrand, P. and Champsaur, P. (2012), "Combination of texture analysis and bone mineral density improves the prediction of fracture load in human femurs", *Osteoporos Int.*, **23**,163-169. https://doi.org/10.1007/s00198-011-1703-1.

Lekadir, K., Hazrati-Marangalou, J., Hoogendoorn, C., Taylor, Z., van Rietbergen, B. and Frangi, A.F. (2015), "Statistical estimation of femur micro-architecture using optimal shape and density predictors", *J. Biomech*., **48**(2015), 598-603. https://doi.org/10.1016/j.jbiomech.2015.01.002.

Maire, J.F. and Chaboche, J.L. (1997), "A new Formulation of continuum damage mechanics (CDM9 for composite materials", *Aerosp. Sci. Technol.*, **1**(4), 247-257. https://doi.org/10.1016/S1270-9638(97)90035-3.

Marco,M., Giner. E., Larrainzar, R., Caeiro, J.R., and Miguelez, M.H. (2017), "Numerical Modelling of Femur Fracture and Experimental Validation Using Bone Simulant", *Ann. Biomed. Eng*., **45**(10), 2395-2408. https://doi.org/10.1007/s10439-017-1877-6.

Mariage, J.F. (2003), "Simulation numérique de l'endommagement ductile en formage de pièces massives", Ph.D. Dissertation, Université de Technologie de Troyes, France.

Marigo, J. J. (1981), "Formulation of a damage law for an elastic material", *Comptes Rendus, Serie II-Mecanique, Physique, Chimie, Sciences de l'Univers, Sciences de la Terre,* **292**(19), 1309-1312.

Milne, I., Robert O. Ritchie, Bhushan Lal Karihaloo (2003), *Comprehensive Structural Integrity*, Elsevier, The Netherlands.

Morgan, E.F., Bayraktar, H.H. and Keaveny, T.M. (2003), "Trabecularbonemodulus– density relationships depend on anatomic site", *J. Biomech*., **36**, 897-904. https://doi.org/10.1016/S0021-9290(03)00071-X.

Nakhli, Z., Ben Hatira, F., Pithioux, M. and Chabrand, P. (2017), "Dépendance de la modélisation par élements finis du fémur humain de la reconstruction tridimensionnelle", *International Congress / Congrès International Design and Modelling of Mechanical Systems Conception et Modélisation des Systèmes Mécaniques*, Hammamet, Tunisia, Mars.

Nawathe, S., Yang, H., Fields, A.J., Bouxsein, M.L. and Keaveny, T.M. (2015), "Theoretical effects of fully ductile versus fully brittle behaviors of bone tissue on the strength of the human proximal femur and vertebral body", *J. Biomech*., **48**, 1264-1269. https://doi.org/10.1016/j.jbiomech.2015.02.066.

Pithioux, M., Chabrand, P., Hochard, C.H. and Champsaur, P. (2011), "Improved Femoral Neck fracture predictions using anisotropic failure criteria models", *J. Mech. Med. Biol.*, **11**(5), 1333-1346. https://doi.org/10.1142/S0219519412004478.

Pituba, J., Fernandes, G.R. and de Sousa Neto, E.A. (2016), "Modeling of cohesive fracture and plasticity processes in composite microstructures", *J. Eng. Mech.*, **142**(10), 1-15. https://doi.org/10.1061/(ASCE)EM.1943-7889.0001123.

Pituba, J.J.C, and Lacerda, M.M.S. (2012), "Simplified damage models applied in the numerical analysis of reinforced concrete structures", Revista *Ibracon de Estruturas e Materiais*, **5**(1), 26-37. http://dx.doi.org/10.1590/S1983-41952012000100004.

Saanouni, K., Forster, Ch., Ben Hatira, F. (1996), "On the Anelastic flow damage", *Int. J. Damage Mech.*, **3**(2), 140-169. https://doi.org/10.1177/105678959400300203.

Sanyal, A. (2013), "Bone Strength Multi-axial Behavior – Volume Fraction, Anisotropy and Microarchitecture", Ph.D. Dissertation, University of California, Berkeley, USA.

Schmidt, J., Henderson, A., Ploeg, H., Deluzio, K. and Dunbar, M. (2006), "Finite element analysis of stem dimensions in a revision total knee arthroplasty using visible human computed tomography data" *14th Annual Symposium on Computational Methods in Orthopaedic Biomechanics*, Chicago IL, USA, March.

Tellache, M., Pithioux, M., Chabrand, P. and Hochard, C. (2009), "Femoral neck fracture prediction by anisotropic yield criteria", *Eur. J. of Comput. Mech. /Rev. Eur. Mec. Num.*, **18**(1), 33-41. https://doi.org/10.3166/ejcm.18.33-41.

Toro, S., Sanchez, P.J., Blanco, P.J., de Souza Neto, E.A., Huespe, A.E. and Feijoo, R.A. (2016), "Multiscale formulation for material failure accounting for cohesive cracks at the macro and micro scales", *J. Plasticity*, **76**(2016), 75-110. https://doi.org/10.1016/j.ijplas.2015.07.001

Varga, P., Schwiedrzik, J., Zysset, Ph. K., Fliri-Hofmanna, L., Widmera, D., Gueorguiev, B., Blauth, M. and Windolf, M. (2016), "Nonlinear quasi-static finite element simulations predict in vitro strength of human proximal femora assessed in a dynamic sideways fall setup", *J. Mech. Behav. Biomed. Mater.,* **57**, 116-127. https://doi.org/10.1016/j.jmbbm.2015.11.026.

Viceconti, M., Taddei, F., Cristofolini, L., Martelli, S., Falcinelli, C. and Schileo, E. (2012), "Are spontaneous fractures possible? An example of clinical application for personalised, multiscale neuro-musculo-skeletal modelling", *J. Biomech.*, **45**(2012), 421-426. https://doi.org/10.1016/j.jbiomech.2011.11.048.

Wang, E., Nelson, T. and Rauch, R. (2004), "Back to Elements-Tetrahedra vs. Hexahedra", International ANSYS Conference Proceedings (2004), Munich, Germany.

Zagane, M.S., Benbarek, S., Sahli, A., Bouiadjra, B.B. and Boualem, S. (2016), "Numerical simulation of the femur fracture under static loading", *Struct. Eng. Mech*., **60**(3), 405-412. http://dx.doi.org/10.12989/sem.2016.60.3.405.

PL